Hot-electron relaxation dynamics in quantum wires

R. Gaška, R. Mickevičius, and V. Mitin
Department of Electrical and Computer Engineering, Wayne State University, Detroit, Michigan 48202

Michael A. Stroscio and Gerald J. Iafrate
U.S. Army Research Office, P.O. Box 12211, Research Triangle Park, North Carolina 27709

H. L. Grubin
Scientific Research Associates Inc., Glastonbury, Connecticut 06033-6058

(Received 16 February 1994; accepted for publication 28 March 1994)

Monte Carlo simulations of hot nonequilibrium electron relaxation in rectangular GaAs quantum wires of different cross sections are carried out. The simulations demonstrate that the initial stage of hot-electron cooling dynamics is determined by cascade emission of optical phonons and exhibits strong dependence on the excitation energy. The second (slow) relaxation stage is controlled by strongly inelastic electron interactions with acoustic phonons as well as by nonequilibrium (hot) optical phonons. The relaxation times obtained in our simulations are in good agreement with the results of recent luminescence experiments. At low electron concentrations where hot phonon effects are negligible the cascade emission of optical phonons may lead to the overcooling of the electron system to temperature below the lattice temperature. These electrons then slowly (during tens of picoseconds) relax to equilibrium due to the interaction with acoustic phonons. At certain excitation energies strong intersubband electron scattering by optical phonons leads to electron redistribution among subbands and intersubband population inversions. If the electron concentration exceeds 10^5 cm^{-1}, hot phonon effects come into play. In contrast to bulk materials and quantum wells, hot phonon effects in quantum wires exhibit strong dependence on the initial broadening of the energy distribution of the electrons. The very initial electron gas relaxation stage in quantum wires is faster in the presence of hot phonons, while for $t>0.5$ ps the hot phonon thermalization time defines the characteristic electron cooling time.

I. INTRODUCTION

Potential possibilities of utilizing unique properties of quasi-one-dimensional (1D) semiconductor structures (peaklike density of states, high packing density, high operation frequencies) for the development of a new generation of electronic and optoelectronic devices have stimulated enhanced interest in investigating the nonequilibrium electron relaxation processes in these structures. Energy dissipation processes of hot electron gases define such characteristics as device operating speed, efficiency, gain, transport characteristics, noise, etc. Although there exist a number of publications dealing with relaxation processes in 1D electron gases,[1–14] the relaxation dynamics of photoexcited carriers under highly nonequilibrium conditions have received less attention. Recent experimental investigations clearly demonstrate different behaviors of photoexcited electron-hole plasmas in 1D and 2D systems.[9–13] Time-resolved luminescence measurements in 1D quantum wires (QWIs)[9–12] indicate that nonequilibrium carrier relaxation to the lowest 1D state is rather slow compared to that measured in quantum wells. Thus, with current interest in developing a new generation of devices based on 1D semiconductor structures it is important to understand the temporal evolution of relaxation of nonequilibrium carriers following initial excitation. This evolution, especially its initial stage (first few picoseconds following pulse excitation), is of great importance for device applications, and, in particular, for high-speed photonic devices. There are several important aspects of electron relaxation in 1D quantum wires to be considered in great detail.

At the operating temperatures of most optoelectronic devices (30–300 K), often the only important energy and momentum relaxation mechanism is the electron-phonon interaction.[4,15] In contrast to 3D or 2D systems, electron-electron pair collisions in QWIs do not affect electron relaxation, whereas electron-phonon interactions remain very strong.[4,16–18] That is why at low electron concentration when the intersubband electron-electron interaction is weak,[4,19] electron scattering by phonons determines the entire electron relaxation dynamics. It appears that phonons in QWIs are far from the same as in bulk materials.[20–22] Along with electron quantization there may exist optical phonon quantization. It has been demonstrated[23] that acoustic phonon scattering in QWIs is essentially inelastic due to the lack of translational symmetry and the resultant uncertainty of momentum conservation. Therefore, in considering the electron dynamic behavior in QWIs it is extremely important to allow for the real phonon spectrum in QWIs.

When electrons are excited well above the bottom of the conduction band they relax via cascade emission of phonons and drive the phonon system out of equilibrium. It is now a commonly accepted notion that nonequilibrium (hot) phonons strongly affect electron transport and relaxation in bulk materials (see, e.g., Ref. 24). Hot phonon effects also explain observations of very slow electron cooling in quantum wells following subpicosecond photoexcitation of hot electrons (see, e.g., Ref. 25). The hot phonon problem in QWIs has been addressed previously in Refs. 2, 6, and 8. However, the kinetic approach used in Ref. 2 does not pro-

 0021-8979/94/76(2)/1021/8/$6.00

vide information about relaxation dynamics, while in Ref. 8 the peculiarities related to 1D nature of nonequilibrium electron-phonon system have been overlooked.

In contrast to 3D or 2D systems, the intrasubband electron-electron pair interaction in QWIs leads only to momentum exchange between interaction indistinguishable electrons and does not contribute to the relaxation process. Hence, at least during initial relaxation stage, the electron gas cannot be described by a Maxwellian distribution function and it is necessary to investigate electron relaxation without any *a priori* assumptions about the electron distribution function.[5,6,8] Moreover, the 1D nature of optical phonons in QWIs results in some specific peculiarities of hot phonon buildup that should strongly modify hot phonon effects in QWIs.[6]

In this paper the simulation of the relaxation of hot nonequilibrium electrons has been carried out allowing for all the specific aspects of electron dynamics in QWIs mentioned above.

II. MODEL AND METHOD

Simulation of hot-electron relaxation has been performed in a rectangular GaAs QWIs embedded in AlAs. We employ an ensemble Monte Carlo technique specially suited for 1D electron simulation.[15] A two-dimensional, infinitely deep square potential well confines electrons in the QWI with a multisubband energy structure. The hot-electron energy dissipation model includes electron interactions with confined longitudinal-optical (LO), localized surface (interface) optical (SO) phonons,[17,18] and bulk-like acoustic phonons[23] as well as nonequilibrium optical phonon populations. We have included inelasticity of electron-acoustic phonon scattering in a QWI in full detail using the technique proposed in Ref. 23. The initial distribution of excited electrons among subbands is considered to be defined by the density of states for a given excess energy in each subband.

We start the simulation of electron relaxation after the initial excitation by a short pulse with a duration of 0.1 ps. We have not simulated electron relaxation in coherent regime ($t<100$ fs) which requires a quantum mechanical description. Instead, we have focused our attention on the time range $t>0.1$ ps when electrons can be treated semiclassically.[26–29] We are interested primarily in peculiarities of the electron-phonon interaction in QWIs. Therefore, we do not take into account the electron-hole interaction. This situation could take place when electrons are photoexcited from near-monoenergetic impurity levels. The initial state for electron relaxation accounts for the broadening of the electron energy distribution due to two effects: (i) uncertainty in electron initial energy due to the short electron average lifetime at the excited level ($\Delta\epsilon\approx10^{-2}$ eV for $\Delta t\approx10^{-13}$ s); (ii) spectral broadening of the exciting pulse with duration of the order of 10^{-13} s. In accounting for these effects we assume that they both lead to a Gaussian distribution of electron energy at $t=t_0$, which corresponds to the end of the excitation pulse. A Gaussian broadening factor is used instead of a Lorentzian (typically incorporated into idealized theoretical models[26,27]) to prevent the unrealistically large spread of electron energies. This approach has been justified for the electron-phonon interaction in a QWIs demonstrating that the Golden Rule formalism may be retained by convolving a Gaussian broadening function containing a constant broadening factor.[30] We vary the excitation energy ϵ_{ex}, which corresponds to the center of a Gaussian distribution, as well as, $\Delta\epsilon$, the half-width of this distribution.

Nonequilibrium phonons have been included by calculating the phonon occupation number versus phonon wave vector (phonon distribution) within the Monte Carlo procedure. In accordance with the 1D nature of optical phonons in QWIs, the increment of phonon occupation number after each emission (sign +) or absorption (sign −) event is given by the term $\pm(2\pi/\Delta q)(n/N)$, where Δq is the step of the grid in q space used to record the N_q histogram, n is the electron concentration per unit length of a QWI, and N is the actual number of particles in the simulation.

In Monte Carlo simulations of bulk and 2D nonequilibrium electron-optical phonon systems, the mesh interval for the phonon occupation number Δq is not a crucial parameter, given that the interval is much less than the q-space region populated by nonequilibrium phonons which can be easily estimated. This is due to the fact that the phonon reabsorption rate depends on the integrated (average) occupancy over the entire region which is not crucially sensitive to the mesh interval. However, in 1D systems as we will see in a due course, the reabsorption rate depends only on the local value of phonon occupancy N_q at an appropriate q value. Therefore, as the mesh interval becomes smaller, both the local occupancy and the reabsorption rate become larger. This problem is particularly important when considering near-monoenergetic electron excitation. There are, of course, physical limits on the magnitude of Δq. These limits follow from the uncertainty in the phonon longitudinal wave number due to the finite length of the QWI.

We have taken a QWI of length $L_x=10$ μm, so that $\Delta q=2\pi/L_x\approx6\times10^3$ cm^{-1}. Hot phonon thermalization due to the decay of optical phonons into acoustic phonons is taken into account by recalculating N_q for every mesh interval at the end of each time step. It has been demonstrated[31] that the phonon thermalization time τ_{ph} in low-dimensional structures depends weakly on the sizes of the structure and is close to the bulk value. For simulations at $T=30$ and 77 K, we have used the value $\tau_{ph}=7$ ps.[24] The time step in our simulations has been chosen to be smaller than the average time between two events of electron scattering by optical phonons and much less than the phonon thermalization time τ_{ph}. We have not taken into account the increase in the acoustic phonon population as a result of the decay of nonequilibrium optical phonons. There are two reasons for this. First, the buildup of nonequilibrium optical phonons occurs only in a very narrow region of the Brillouin zone (near the zone center), so that over the entire zone the average occupation number increases only negligibly. This is true for systems of any dimensionality since the electrons interacting with phonons populate only the center region of the Brillouin zone. Second, the acoustic phonons in QWIs embedded in surrounding materials with similar elastic properties (GaAs in AlAs in our case) may penetrate through GaAs/AlAs interfaces and escape from the QWI. Therefore, we have ex-

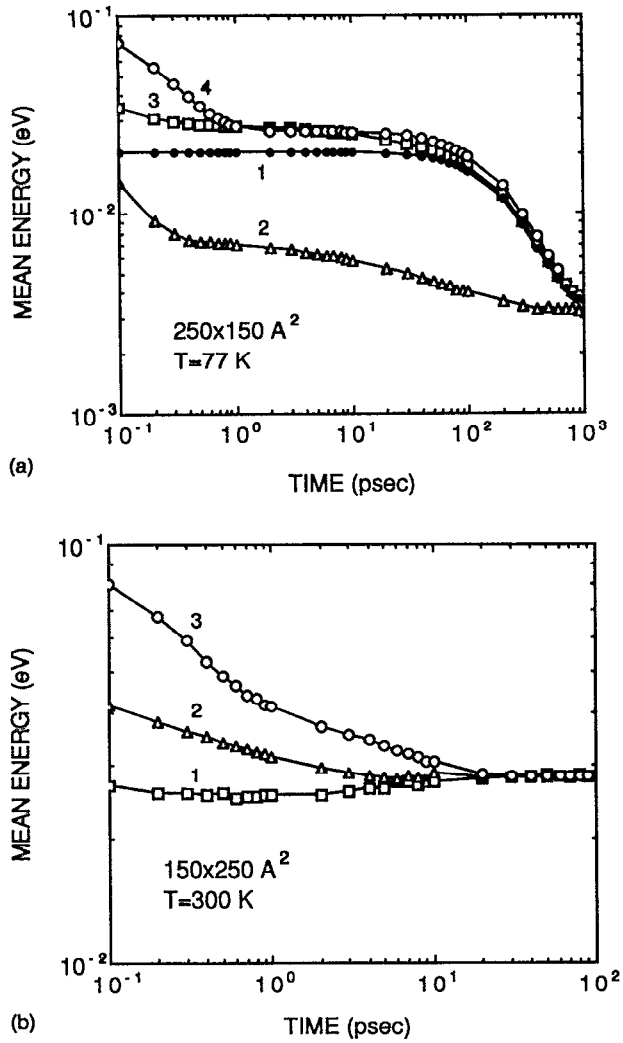

FIG. 1. Time evolution of the mean-electron energy in a QWI with cross section 150×250 Å^2 after excitation at two lattice temperatures: (a) $T=77$ K and (b) $T=300$ K. Curve 1 in (a) corresponds to electron excitation energy $\epsilon_{ex}=20$ meV; 2, 42 meV; 3, 67 meV; 4, 100 meV. In (b) 1, 42 meV; 2, 67 meV; 3, 100 meV.

cellent thermal conductivity and the QWI should not be heated much more than the whole GaAs/AlAs structure. Given that the surrounding AlAs is sufficiently massive, the increase in temperature would be negligible even if the QWI strongly radiates acoustic phonons.

III. RESULTS AND DISCUSSION

A. Low electron concentrations

Let us first consider electron concentrations less than 10^5 cm^{-1} where nonequilibrium phonon effects can be neglected.

Calculations with various excitation energies show that in the time scale of 10^{-9} s electron relaxation exhibits one or two distinguishable stages. Figure 1 demonstrates the electron cooling dynamics in a QWI with cross section 150×250 Å^2 for lattice temperatures of $T=77$ K and $T=300$ K, as well as for different electron excitation energies ϵ_{ex} counted from the bottom of the lowest conduction subband. The mean electron energy plotted on the vertical axis in Figs. 1(a) and 1(b) is calculated relative to the bottom of the first subband. Thus it consists of two parts: the kinetic energy corresponding to one degree of freedom in a QWI and the intersubband separation energy. The electron excitation energy ϵ_{ex} has been varied from 20 to 100 meV. This implies that for this particular cross section of the QWI, up to the three lowest subbands can be occupied by electrons at the initial time, $t=0$. One can see from Fig. 1(a) that for electron excitation at 20 meV, the electron gas cooling is slow ("slow" stage). The "fast" stage in the mean electron energy dependence on time is observed when electrons are excited above the optical phonon energy ($\hbar w_{LO}$ or $\hbar w_{SO}$, where $\hbar w_{LO}$ and $\hbar w_{SO}$ are energies of LO and SO phonons, respectively). Electrons initially (in the subpicosecond time scale) cool down losing their energy due to the interaction with optical phonons. Since the optical phonon absorption events at temperature $T=77$ K are negligibly rare, the electron gas relaxation dynamics is determined by the emission of optical phonons with characteristic times $\tau_{e-LO}\approx10^{-13}$ s and $\tau_{e-SO}\approx10^{-12}$ s (for electron-LO and electron-SO phonon interaction, respectively). It is worth to mention that ultrafast nonequilibrium carrier relaxation with characteristic cooling times of the same order of magnitude have been experimentally observed in time-resolved photoluminescence and cathodoluminescence measurements.[9,11,12] At low optical excitation levels the sharp line of band-edge photoluminescence occurs during the laser excitation.[9,12] This implies that hot carriers lose the major portion of their excess energy during the time much shorter than the excitation pulse of 25 ps. The analysis of low-temperature cathodoluminescence spectra suggests that carrier capture and relaxation to the bottom subbands in GaAs QWIs grown on nonplanar substrates occurs in a subpicosecond time scale.[11] At a lattice temperature of $T=300$ K the electron cooling dynamics is influenced strongly by optical phonon absorption which reduces the electron gas cooling rate [Fig. 1(b)].

The duration of the "fast" relaxation stage as well as the entire electron gas cooling dynamics for $\epsilon_{ex}>\hbar w_{LO}$ exhibits a strong dependence on the excitation energy. As discussed below, when electrons are excited just above the LO phonon energy they cool down to the bottom of the first subband on a subpicosecond time scale [curve 2 in Fig. 1(a) and curve 1 in 1(b)]. Electrons emit optical phonons and occupy states near the subband bottom. Therefore, the mean electron energy drops below that for $\epsilon_{ex}=20$ meV [curve 1 in Fig. 1(a)]. For a lattice temperature of $T=300$ K we observe anomalous cooling dynamics when electrons occur below the thermal equilibrium energy [curve 1 in Fig. 1(b)]. Overcooling of the electron gas occurs if the electron excitation energy falls into the range $\hbar w_{LO}<\epsilon_{ex}<\hbar w_{LO}+k_BT/2$, where $k_BT/2$ is the electron kinetic energy at a given temperature T corresponding to one degree of freedom in a QWI. At lower temperatures ($T=77$ K) the transient electron overcooling disappears because the chosen broadening of electron initial energy distribution exceeds the electron thermal equilibrium energy $k_BT/2$.

The "slow" stage of electron relaxation is controlled by the electron interaction with acoustic phonons. Our calculations demonstrate that electron gas thermalization process in a QWI of cross section of 150×250 Å^2 lasts about 1 ns at a

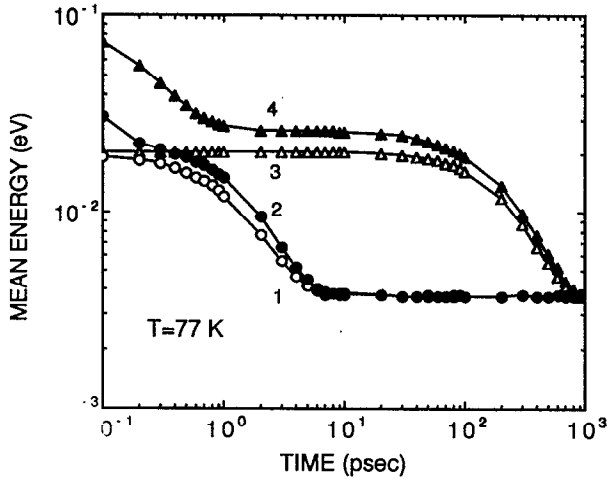

FIG. 2. Time evolution of mean-electron energy after excitation for QWIs with two different cross sections: 40×40 Å^2 (curves 1 and 2); 150×250 Å^2 (curves 3 and 4). Curves 1 and 3 correspond to excitation energy ϵ_{ex}=20 meV; 2 and 4, 100 meV. The lattice temperature is T=77 K.

lattice temperature T=30 K [Fig. 1(a)], and 30 ps at T=300 K [Fig. 1(b)]. This time depends strongly not only on the lattice temperature but also on the cross section of a QWI as does the acoustic phonon scattering rate.[23] The role of acoustic phonon scattering is demonstrated in Fig. 2 for electron cooling dynamics in a QWI with a cross section 40×40 Å^2 compared with the cooling dynamics in a 150×250 Å^2 QWI. The electron energy relaxation due to the interaction with acoustic phonons is much faster in the thin QWI as a result of two factors: (i) the acoustic phonon scattering rate is roughly inversely proportional to the cross section of a QWI, and (ii) the inelasticity of the electron-acoustic phonon interaction also increases with the decrease of the cross section.[23]

The relaxation times of the same order of magnitude have been derived from the time-resolved photoluminescence measurements at low excitation levels.[12] After initial hot-carrier relaxation below optical phonon energy, the further evolution of the band-edge luminescence line shape is characterized by the time of the order of hundreds of picoseconds.[12] Therefore, the electron-acoustic phonon interaction might be responsible for the time evolution of luminescence spectra. Rough estimates yield electron thermalization time due to interaction with acoustic phonons of the order of 500 ps for the structure parameters and temperature (T=5 K) of Ref. 12.

One can see from Fig. 1(a) and Fig. 1(b) that the electron thermal equilibrium energy for T=300 K is larger than could be expected from $k_BT/2\approx$13 meV, while for T=77 K it practically coincides with $k_BT/2$=3.3 meV. The difference in thermal equilibrium energies comes from the calculation of the electron mean energy in QWIs with multisubband energy structure. Approximately one third of electrons occupy upper subbands in the equilibrium state at a lattice temperature T=300 K due to the Boltzmann distribution. The mean electron energy includes the electron gas kinetic energy ($k_BT/2$) of free motion along the wire and the energy representing the spatial quantization (separation between subbands) in two

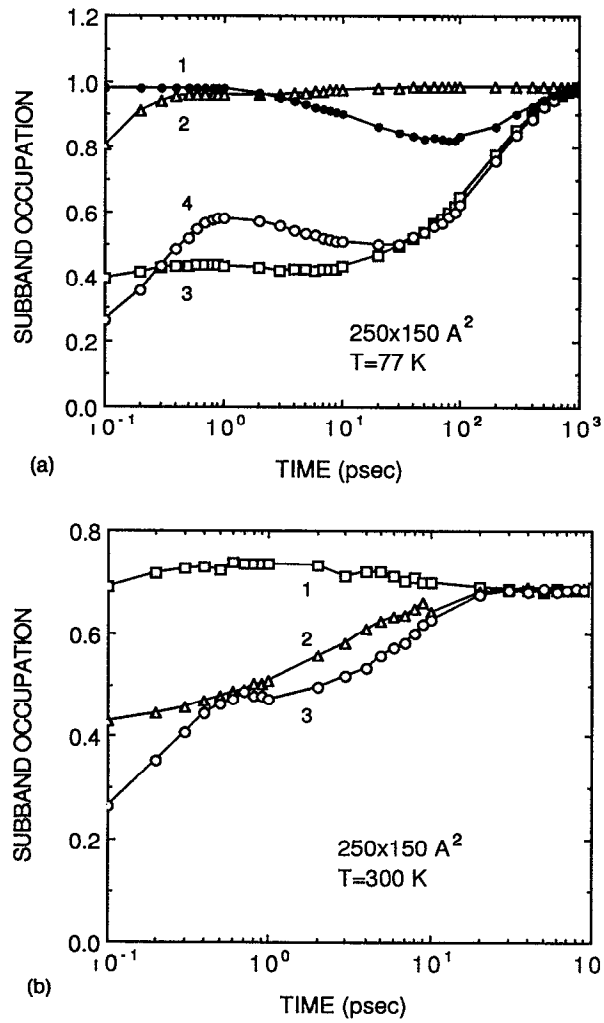

FIG. 3. Time evolution of the occupancy of the first subband for the same structure parameters and excitation energies in Fig. 1; (a) T=77 K, (b) T=300 K.

other directions. In the extreme limit of thick QWIs, when a large number of subbands becomes occupied, the electron mean energy tends to $3k_BT/2$ corresponding to the 3D electron gas.

Simulation of hot-electron relaxation dynamics in QWIs demonstrates that intersubband electron scattering primarily by optical phonons leads to a significant carrier redistribution among subbands (Fig. 3). When electrons are excited well above the bottom of the second subband (ϵ_{ex}=100 meV) multiple electron transitions between various subbands due to interaction with optical phonons lead to a nonmonotonous time dependence of the relative occupancy of the first (lowest) subband [curves 3 in Figs. 3(a) and 3(b)]. Acoustic phonon scattering is also responsible for electron intersubband transitions. For the case where the cross section is 150×250 Å^2, the separation between the first and the second subband is less than the optical phonon energy, so that electrons cannot be scattered from the bottom of the second subband by the emission of optical phonons. Accordingly, at low temperatures electrons can be "trapped" in the second subband. They are slowly (with characteristic time of tens and hundreds of picoseconds) released from it due to intersubband

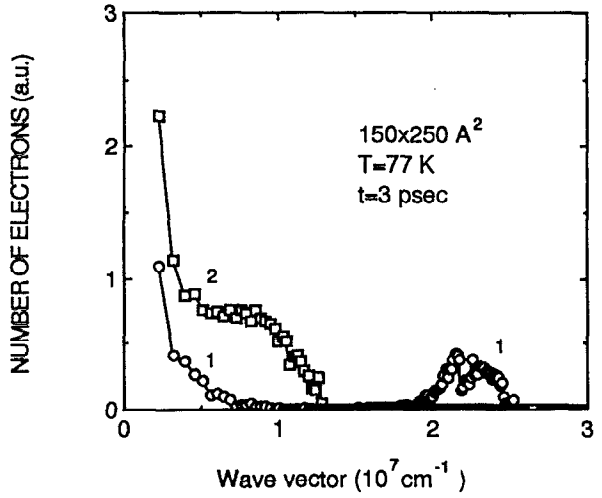

FIG. 4. Electron distribution in momentum space in a QWI with cross section 150×250 Å^2 3 ps after excitation with ϵ_{ex}=67 meV. Curve 1 represents the electron distribution in the first (lowest) subband; curve 2 represents the second subband. The lattice temperature is T=77 K.

electron scattering by acoustic phonons [curves 3 and 4 in Fig. 3(a)]. In this case the second subband serves as a hot-electron reservoir and significantly slows electron cooling. Even in the case when most electrons are excited into the first subband (ϵ_{ex}=20 meV), a small fraction of them (from the high-energy tail of the Gaussian excitation energy distribution) are initially scattered by acoustic phonons to the second subband and then return to the first one [curve 1 in Fig. 3(a)]. The energy of the plateau [curve 3 in Fig. 1(a)] virtually coincides with the position of the second subband with respect to the first subband bottom (27 meV) indicating that electrons are "trapped" there. At high temperatures [T=300 K, Fig. 3(b)] electrons "escape" from the upper subbands due to intersubband absorption of optical phonons as well as stronger intersubband acoustic phonon scattering, and reach an equilibrium distribution among subbands in 30 ps.

Under certain excitation conditions intersubband electron scattering by optical phonons may lead to intersubband population inversion. We observe an intersubband population inversion when two conditions are met: (i) separation between two lowest subbands in the QWI is less than minimum optical phonon (LO or SO) energy, so that electrons cannot be scattered from the bottom of the second subband by the emission of optical phonons (we demonstrate results for a QWI with cross section 150×250 Å^2, where this condition is fulfilled); (ii) electrons are excited just above characteristic energy $\epsilon=\epsilon_{12}+\hbar w_{LO}$, where ϵ_{12} is the energy of the bottom of the second subband. Due to a significant difference in the number of final states (peak-like density of states near each subband bottom) electrons from both the first and the second subbands are scattered predominantly into the second subband bottom after the emission of LO phonons. Thus, the number of electrons at the bottom of the second subband exceeds the number of electrons at the bottom of the first subband and a strong intersubband population inversion occurs near the center of the Brillouin zone (k=0). Figure 4 presents the distribution of electrons in momentum space for the two lowest subbands 3 ps after excitation. Electrons in the first subband are still hot (wave numbers $k>2\times10^7$ cm^{-1} on curve 1 in Fig. 4) after emission of optical phonons and they relax to the bottom of the subband by interacting with acoustic phonons. Electrons in the second subband occupy states with smaller wave vectors near the subband bottom. This population inversion near the center of the Brillouin zone (k=0) lasts about 10 ps at a lattice temperature of T=77 K. This time is defined by intrasubband and intersubband electron scattering by acoustic phonons. Intersubband electron scattering by acoustic phonons is responsible for electron release from the second subband at low temperatures where optical phonon absorption is virtually frozen out, while intrasubband acoustic phonon scattering leads to the thermalization of the electron distribution. As one can see from Fig. 4 the population inversion at small electron wave vectors is reduced due to presence of some fraction of electrons near the bottom of the first subband. The number and energy of these electrons depend strongly on the excitation regime. Due to the Gaussian electron excitation energy distribution some electrons from the high-energy tail can emit two optical phonons and cool down to the bottom of the first subband. Thus, as the electron initial energy broadening increases, the occupation of states with small wave vector in the first subband also increases, and the effect of population inversion decreases.

B. Hot phonon effects

Due to optical phonon quantization and the resultant 1D momentum conservation in quantum wires, electrons can emit or absorb optical phonons with wave vectors which are strictly defined by the electron momentum and the phonon energy. In general, the phonon wave number is defined by the energy and momentum conservation equations and is given by

$$q=\sqrt{k^2+k'^2-2kk'\cos\theta}\,, \tag{1}$$

where k is the electron wave number before scattering, $k'=\sqrt{k^2\pm 2m^*\omega_0/\hbar}$ is the electron wave number after absorption (sign +) or emission (sign −) of the optical phonon of frequency ω_0, and θ is the angle between electron wave vectors before and after scattering. In 1D structures there are just two final states for scattered electrons: forward scattering with $\cos\theta=1$ or backward scattering with $\cos\theta=-1$. Consequently, there are two possible phonon wave vectors available for emission (and two for absorption) by any single electron:

$$q_1=|k-k'|,\quad q_2=|k+k'|\,. \tag{2}$$

In contrast, in quantum wells (or bulk materials) due to existence of additional degree(s) of freedom, $\cos\theta$ can take any value in the range $(-1,+1)$, so that there is an entire range of a phonon q values from $|k-k'|$ to $k+k'$ available for electron interactions.

Therefore, electrons in QWIs having appreciably different energies generate nonequilibrium phonons in different narrow q-space regions which do not overlap. In turn, these phonons can be reabsorbed only by the electrons that have generated them, unlike in bulk materials and in quantum

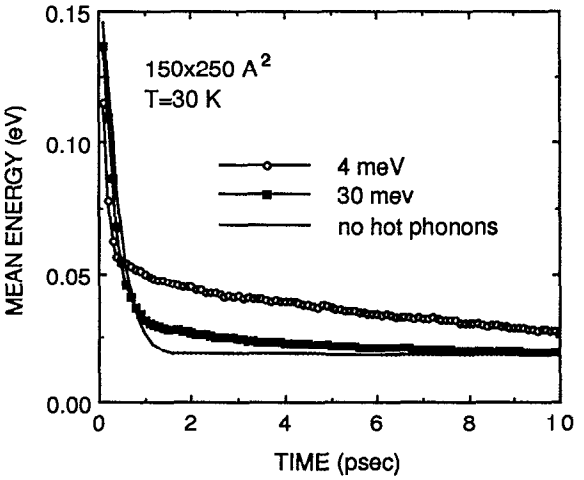

FIG. 5. Mean-electron energy as a function of time after initial electron excitation at an energy equal to 4.5 times the LO phonon energy, for two initial widths of the electron energy distribution. Electron concentration is $n=10^5$ cm^{-1} and lattice temperature is $T=30$ K. Solid curves describe the energy evolution for the case of an equilibrium phonon distribution. Results apply to the case of a single-subband QWI neglecting SO phonons.

wells where electrons can reabsorb phonons emitted by other electrons. Consequently, electrons which have different energies cannot interact through the emission and subsequent reabsorption of optical phonons. Thus, electrons and the phonons associated with them (with appropriate wave vectors) are isolated from other electron-phonon pairs if electrons are in different states. Thus, for 1D structures we eliminate one cross-correlation effect which is always present in the nonequilibrium electron-phonon system in bulk materials and in quantum wells and which is important when considering electric noise.[32]

Another consequence of the 1D nature of the electron-phonon interaction in QWIs is that the reabsorption probability for each single electron in the QWI does not depend on the integrated phonon occupation number but only on the local occupancy at a certain q. This reabsorption probability decreases as the phonon distribution spreads over q space (given that the integrated occupancy is defined by the concentration of excited electrons and remains constant). The spread of the nonequilibrium phonon population in q space results from the broadening of the electron energy distribution. As a result, the reabsorption rate and hot phonon effects depend strongly on the energy distribution of excited electrons.

Let us first consider a simplified picture in which there is only one energy subband and SO phonons are neglected; that is, only LO and acoustic phonons are present in the QWI. This simplified picture allows us to refine the pure 1D effect of the broadening of the electron energy distribution on the buildup of hot phonons and, hence, on electron cooling dynamics. Figure 5 illustrates electron cooling dynamics in a 150×250 Å^2 QWI at $T=30$ K following initial electron excitation at an energy 4.5 times the LO phonon energy for two different Gaussian electron distribution half widths: 30 and 4 meV. For comparison, we plot the electron relaxation dynamics without nonequilibrium optical phonons. When hot phonons are neglected the cooling dynamics displays two distinguishable stages: the fast stage (with subpicosecond duration) due to the cascade emission of optical phonons, and the second, slow stage of electron thermalization due to interactions with acoustic phonons. It must be noted, however, that in the given time scale of 10 ps, acoustic phonon scattering does not visibly influence the electron relaxation dynamics in this QWI with a rather large cross section of 150 ×250 Å^2. As one can see from Fig. 5 the very initial relaxation stage ($t<0.5$ ps) is faster in the presence of hot phonons. The higher nonequilibrium phonon populations are created (4 meV), the faster is the very initial relaxation stage. This effect can be understood if one first considers the temperature dependence of the relaxation rate. At high temperatures both the emission and absorption rates are higher. This leads to fast energy redistribution of excited electrons. The cooling rate of electrons which emit optical phonons increases and that of electrons which absorb phonons decreases because of the $\epsilon^{-1/2}$ energy dependence of 1D density of states and scattering rates. The increase, however, is faster than the decrease due to the same $\epsilon^{-1/2}$ function. Therefore, the total 1D electron gas cooling rate increases when the electron energy redistributes due to emission and absorption of optical phonons. At very high temperatures this happens on a very short time scale while electron distribution at low temperatures still remains unchanged. Hence, the very initial electron cooling rate in QWIs increases when increasing the lattice temperature, provided that electrons are excited well above optical phonon energy and thermal equilibrium energy. (Note that in bulk materials, where the emission and absorption rates increase with energy the relaxation rate is higher at low lattice temperatures. There should be no temperature dependence of the initial relaxation rate in 2D systems.) To observe an appreciable temperature effect on the relaxation rate it is necessary that phonon occupation number be greater than 1. Under phonon equilibrium such occupation numbers could even be unachievable in a solid state. However, due to strong buildup of nonequilibrium phonons at high excited electron concentrations the occupation number for certain phonon modes may be considerably higher than 1. This is why the initial relaxation is faster for higher nonequilibrium phonon occupations and thus, for narrower initial electron energy distributions (Fig. 5).

One can see from Fig. 5 that the onset of hot phonons leads to a substantial reduction of the electron gas cooling rate for $t>0.5$ ps due to strong reabsorption of nonequilibrium phonons. The onset of hot phonons occurs sooner if the electron energy distribution is narrower (4 meV). Hence, electron cooling is slower for narrow electron distributions. The effect of narrowing of the electron energy distribution is similar to that of increasing the electron concentration and, as we have already discussed, it is a purely 1D effect. As has been demonstrated in a previous subsection, in QWIs with small cross sections (40×40 Å^2) the acoustic phonon scattering rate is higher and this scattering is much more inelastic than in QWIs with large cross sections (150×250 Å^2). Therefore, in a QWI with a 40×40 Å^2 cross section, acoustic phonon scattering is a very effective energy dissipation mechanism and it is responsible for fast relaxation and

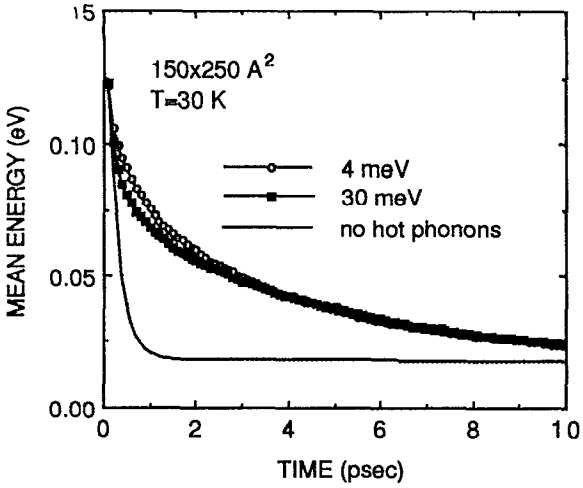

FIG. 6. Mean electron energy vs time for a realistic multisubband QWI structure with both LO and SO optical modes included as well as acoustic phonons. Electron concentration is equal $n=10^6$ cm^{-1}, other parameters and conditions are the same as in Fig. 5.

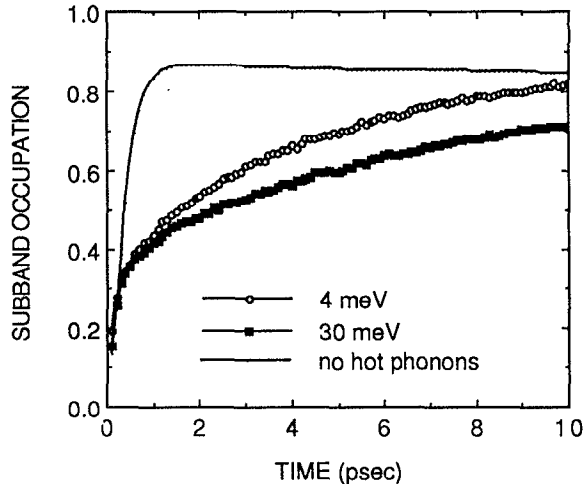

FIG. 7. Time evolution of the relative occupation of the first (lowest) subband. Parameters are the same as in Fig. 6.

smearing out the effect of the initial broadening of the electron distribution on the cooling rate.

We have also considered the realistic case where the multisubband structure of the QWI is taken into account along with all possible optical phonon modes (LO and SO). Figure 6 shows the electron cooling dynamics in this realistic structure for 4 and 30 meV electron excitation linewidths. The dependence of hot phonon buildup on the electron distribution broadening is washed out almost completely in this realistic structure due to various intrasubband and intersubband transitions assisted by the LO and the two SO modes. The reason is that nonequilibrium phonon peaks in q space in this case overlap and form a complex broad distribution in q space virtually independent of initial electron distribution. The main effect which comes into play within this realistic model is the dependence of the number of the upper subbands involved in electron cooling on the initial electron energy distribution. Figure 7 demonstrates the time evolution of the subband filling by electrons. In the case of a broad electron initial distribution (30 meV) there are more subbands occupied by electrons scattered from the high-energy tail. Therefore, the return of electrons to the first subband is slower than for a narrow electron distribution (4 meV). Hot phonons lead to stronger intersubband electron redistribution and slower return to the lowest subband. By comparing Figs. 6 and 7 one notices that the different occupation of subbands for 4 and 30 meV excitation linewidths virtually does not affect the mean-electron energies which coincide for both excitation regimes after 3 ps following excitation. This, at the first glance, strange behavior is related to the fact that the electron kinetic energy related to 1D free motion in each subband is higher for 4 meV excitation linewidth due to stronger hot phonon effects. This difference in kinetic energies is compensated by the higher occupation of the upper subbands in the case of a 30 meV linewidth. Consequently, the 4 meV curve in Fig. 6 contains a larger part of kinetic energy and a smaller part of "potential" energy than the 30 meV curve.

IV. SUMMARY

Simulation reveals complex dependence of hot-electron gas cooling dynamics on excitation energy, lattice temperature, and structure parameters of QWI. Electron relaxation in subpicosecond time scale is controlled by their interaction with confined optical phonons, whereas thermalization of the electron distribution is defined by essentially inelastic electron-acoustic phonon scattering. Electron gas thermalization is much faster in a thinner QWI due to higher acoustic-phonon scattering rate and stronger inelasticity of electron-acoustic phonon interaction. The relaxation times obtained in our simulations are in good agreement with the results of optical measurements.[9,11,12]

Variation of the initial electron energy substantially changes the entire picture of hot-electron relaxation due to the interaction of electrons with various phonons in QWIs. Calculations demonstrate potential possibilities of two effects: electron gas overcooling and dynamic intersubband population inversion. Both effects exhibit strong dependence on the lattice temperature.

Population inversion is well pronounced at low temperatures, whereas electron gas overcooling benefits from high temperatures. At low temperatures electrons can be "trapped" in the upper subbands below the optical phonon energy and stay there for quite a long time defined by intersubband electron-acoustic phonon interaction.

We have found that hot phonon effects in QWIs are well pronounced for electron concentrations equal to or higher than 10^5 cm^{-1} and depend strongly on the energy distribution of excited electrons. Hot phonon effects become weaker as the broadening of the excited electron energy distribution increases. This result is in complete contrast to the case of bulk materials and quantum wells where the energy distribution of excited electrons virtually does not affect the buildup of nonequilibrium phonons and the reabsorption rate.

ACKNOWLEDGMENTS

The work was supported by the U.S. Army Research Office, the National Science Foundation, and the Center for Compound Semiconductor Microelectronics of the University of Illinois at Urbana-Champaign.

[1] V. B. Campos and S. Das Sarma, Phys. Rev. B **45**, 3898 (1992).
[2] V. B. Campos, S. Das Sarma, and M. A. Stroscio, Phys. Rev. B **46**, 3849 (1992).
[3] D. Jovanovic, J. P. Leburton, K. Ismail, J. M. Bigelow, and M. H. Degani, Appl. Phys. Lett. **62**, 2824 (1993); J. P. Leburton, S. Briggs, and D. Jovanovic, Superlattice Microstructure **8**, 209 (1990).
[4] I. Vurgaftman and J. Singh, Appl. Phys. Lett. **62**, 2251 (1993).
[5] R. Gaška, R. Mickevičius, V. Mitin, and H. L. Grubin, Semicond. Sci. Technol. (to be published, 1994).
[6] R. Mickevičius, R. Gaška, V. Mitin, M. A. Stroscio, and G. J. Iafrate, Semicond. Sci. Technol. (to be published, 1994).
[7] I. Vurgaftman and J. Singh, Semicond. Sci. Technol. (to be published, 1994).
[8] L. Rota, F. Rossi, P. Lugli, and E. Molinari, Semicond. Sci. Technol. (to be published, 1994).
[9] R. Cingolani, H. Lage, L. Tapfer, D. Heitmann, and K. Ploog, Semicond. Sci. Technol. **7**, B287 (1992).
[10] A. C. Maciel, J. F. Ryan, R. Rinaldi, R. Cingolani, M. Ferrara, U. Marti, D. Marrtin, F. Morier-Gemoud, and F. K. Reinhart, Semicond. Sci. Technol. (to be published, 1994).
[11] J. Christen, M. Grundmann, E. Kapon, E. Colas, D. Hwang, and D. Bimberg, Appl. Phys. Lett. **61**, 1611 (1992).
[12] R. Cingolani, R. Rinaldi, M. Ferrara, G. C. La Rocca, H. Lage, D. Heitmann, K. Ploog, and H. Kalt, Phys. Rev. B **48**, 14331 (1993).
[13] A. Endoh, H. Arimoto, Y. Sugiyama, H. Kitada, and S. Muto, Appl. Phys. Lett. **64**, 449 (1994).
[14] R. Cingolani, R. Rinaldi, M. Ferrara, G. C. La Rocca, H. Lage, D. Heitmann, K. Ploog, and H. Kalt, Semicond. Sci. Technol. (to be published, 1994).
[15] R. Mickevičius, V. Mitin, K. W. Kim, and M. A. Stroscio, Semicond. Sci. Technol. **7**, B299 (1992).
[16] H. Sakaki, Jpn. J. Appl. Phys. **19**, L735 (1980).
[17] K. W. Kim, M. A. Stroscio, A. Bhatt, R. Mickevičius, and V. V. Mitin, J. Appl. Phys. **70**, 319 (1991).
[18] R. Mickevičius, V. Mitin, K. W. Kim, M. A. Stroscio, and G. J. Iafrate, J. Phys. Condens. Matter **4**, 4959 (1992).
[19] Yu. M. Sirenko and P. Vasilopoulos, Phys. Rev. B **46**, 1611 (1992).
[20] N. Mori and T. Ando, Phys. Rev. B **40**, 6175 (1989).
[21] H. Rücker, E. Molinari, and P. Lugli, Phys. Rev. B **44**, 3463 (1991).
[22] P. A. Knipp and T. L. Reinecke, Phys. Rev. B **45**, 9091 (1992).
[23] R. Mickevičius and V. Mitin, Phys. Rev. B **48**, 17194 (1993).
[24] R. Mickevičius and A. Reklaitis, J. Phys. Condens. Matter **1**, 9401 (1989).
[25] D. J. Westland, J. F. Ryan, M. D. Scott, J. I. Davies, and J. R. Riffat, Solid-State Electron. **31**, 431 (1988).
[26] A. V. Kuznetsov, Phys. Rev. B **44**, 8721 (1991).
[27] T. Kuhn and F. Rossi, Phys. Rev. B **46**, 7469 (1992).
[28] C. J. Stanton, A. V. Kuznetsov, and C. S. Kim, Semicond. Sci. Technol. (to be published, 1994).
[29] J. Schilp, T. Kuhn, and G. Mahler, Semicond. Sci. Technol. (to be published, 1994).
[30] J. P. Leburton and D. Jovanovic, Semicond. Sci. Technol. **7**, B202 (1992).
[31] G. Mahler, A. M. Kriman, and D. K. Ferry (unpublished).
[32] P. Bordone, L. Varani, L. Reggiani, and T. Kuhn, in *AIP Conference Proceedings on Noise in Physical Systems and 1/f Fluctuations*, St. Louis, MO, 1993 (AIP, New York, 1993), p. 657.